

University of Arkansas, Fayetteville  
**ScholarWorks@UARK**

---

Electrical Engineering Undergraduate Honors  
Theses

Electrical Engineering

---

5-2014

# The synthesis and characterization of copper indium sulfide and cadmium selenide nanocrystals and their applications in photodetectors

Zachary T. Bever

*University of Arkansas, Fayetteville*

Follow this and additional works at: <http://scholarworks.uark.edu/eleguht>

---

## Recommended Citation

Bever, Zachary T., "The synthesis and characterization of copper indium sulfide and cadmium selenide nanocrystals and their applications in photodetectors" (2014). *Electrical Engineering Undergraduate Honors Theses*. 30.  
<http://scholarworks.uark.edu/eleguht/30>

This Thesis is brought to you for free and open access by the Electrical Engineering at ScholarWorks@UARK. It has been accepted for inclusion in Electrical Engineering Undergraduate Honors Theses by an authorized administrator of ScholarWorks@UARK. For more information, please contact [scholar@uark.edu](mailto:scholar@uark.edu).

This thesis is approved.

Thesis Advisor:

*Omaj Manaseh*

Thesis Committee:

---

---

The Synthesis and Characterization of CuInS<sub>2</sub> and CdSe Nanocrystals and  
their Applications in Photodetectors

An Undergraduate Honors College Thesis

in the

Department of Electrical Engineering  
College of Engineering  
University of Arkansas  
Fayetteville, AR

by

Zachary Thomas Bever

## **Abstract**

Semiconductor nanocrystals are a topic of much interest in electrical engineering. Their use has been explored for many applications. This paper investigates the synthesis and characterization of CuInS<sub>2</sub> and CdSe nanocrystals. As the nanocrystals were left in reaction for increasing amounts of time, the bandgap of the material decreased as the nanocrystal size increased due to the quantum confinement effect. The CdSe nanocrystals were then investigated in a photodetector application which achieved a detectivity on the order of  $10^9 \text{ cmHz}^{1/2}\text{W}^{-1}$ .

## **Acknowledgments**

I would like to first thank Dr. Manasreh for the incredible experience of working in his lab for the last two years. It is amazing to think about how much I have learned in my time in his lab. His support and encouragement throughout my academic career has been greatly appreciated and is not taken for granted. I would also like to thank the other students who have been a part of that lab for their kindness and generosity in offering their assistance and insights: Juan Aguilar, Ahmad Nusir, Ramesh Vasan, Scott Mangham, Seung-Yong Lee, Rick Eyi, Jony Sarker, and Yahia Makableh.

## **Table of Contents**

I. Background.....	1
II. Methods.....	2
A. Synthesis of the CdSe Nanocrystals.....	3
B. Synthesis of the CuInS <sub>2</sub> Nanocrystals .....	4
C. Characterization of the Nanocrystals .....	5
D. Applications: Fabrication of a Nanocrystals-Based Photodetector.....	10
III. Conclusions.....	13
IV. Works Cited.....	14

## Table of Figures

Figure 1. Experimental set-up for synthesis .....	4
Figure 2. Samples extracted from reaction at various times .....	5
Figure 3. Samples from Figure 1 under Exposure to UV Light.....	6
Figure 4. Absorbance spectra of samples taken at different reaction times.....	6
Figure 5. Absorbance and photoluminescence spectra .....	7
Figure 6. Absorbance of CdSe nanocrystals taken at different points in reaction .....	8
Figure 7. Photoluminescence spectra of CdSe nanocrystals.....	9
Figure 8. Photodetector Design.....	10
Figure 9. I-V curves for 5 and 50 micron channel photodetectors .....	11
Figure 10. Detectivity of 5 $\mu\text{m}$ and 50 $\mu\text{m}$ photodetectors.....	12

## **I. Background**

The field of nanocrystal semiconductors and their applications is an exciting research topic in electrical engineering, and as such, it has been the focus of many research efforts. The use of nanocrystals is appropriate in many of the same applications for which the bulk semiconductors are used. As such, semiconductor nanocrystals have been investigated to examine their usefulness in applications such as photovoltaic solar cells, light emitting diodes, and photodetectors (Nusir, 2014).

In some instances, the nanocrystals are even better suited for a task than the bulk material because the nanocrystals offer some exciting benefits not matched by bulk semiconductors. For example, nanocrystals can be fabricated and dispersed in solution, offering the benefit of effective mass production. Additionally, the bandgap of nanocrystals grown by wet chemical synthesis – yielding a colloidal solution – can be fine-tuned to match the needs of the current application (Nusir, 2014).

The applications dependent upon the fine-tuning of the bandgap of the semiconductor nanocrystals take advantage of the quantum confinement effect. When the diameter of a nanocrystal formed during synthesis is sufficiently small (on the nanometer scale), the quantum confinement effect dominates (Credi, 2012). As such, the nanoparticle experiences an energy quantization because only specific, discrete energy values are possible for the nanoparticle, and these energy levels can be approximated by using the particle in a box example. As the energy levels become discretized, the bandgap becomes size dependent, and since the size of the nanocrystal can be controlled to a certain extent through the reaction conditions, the scientist also has a measure of control over the bandgap of the nanocrystals. As the size of the nanocrystals increases, the bandgap of the material decreases.



Cadmium selenide is one of the most widely studied nanocrystal semiconductors in optoelectronics. As a direct bandgap material, cadmium selenide is suitable for applications involving the emission, detection, or capture of photons. Cadmium selenide is a binary, II-VI semiconductor. The material is an n-type semiconductor, and in its bulk form has a bandgap of 1.73 eV. The bandgap of CdSe corresponds to the visible to near-infrared region of the electromagnetic spectrum. The nanocrystals can be formed in both CdSe-ZnS core-shell or CdSe (core only) arrangements (Booth, 2012).

Copper indium disulfide ( $\text{CuInS}_2$ ) nanocrystals are an alternative to CdSe nanocrystals. One of their primary benefits over the CdSe nanocrystals is a greatly improved safety factor. The production of  $\text{CuInS}_2$  is much safer because the chemical precursors are safer. Both cadmium and selenium are tremendously dangerous to handle, and great efforts must be made to ensure the safety of those working with their compounds. According to the United States Environmental Protection Agency, repeated contact with even small amounts of cadmium can lead to kidney damage and breathing in high doses of cadmium can damage the lungs and cause death (EPA, 2000). Likewise, acute exposures to selenium compounds via inhalation can cause severe respiratory problems (EPA, 2000).  $\text{CuInS}_2$  is a direct bandgap material, and the bulk bandgap is 1.53 eV which lies in the near infrared region (Booth, 2012).

## **II. Methods**

The purpose of this project is to grow semiconductor nanocrystals, characterize them, and explore potential applications for their use in electrical engineering – in this case, a nanocrystal based photodetector. This can loosely be broken into four steps: nanocrystal synthesis, characterization, and finally measurement of the performance of the photodetector.

## A. Synthesis of the CdSe Nanocrystals

The preparation of the cadmium selenide nanocrystals is an involved multistage process, and much care must be taken at each step in order to ensure that the appropriate compounds are being synthesized. In literature concerning the production of cadmium selenide nanocrystals, the nanocrystals were formed in reactions performed in nitrogen gas ( $N_2$ ) atmosphere at high temperatures (Searson, 2008). These processes were modified slightly to develop a synthesis process. The first step was to prepare the selenium compound to be used in the reaction. To do this, 4 mmol of selenium powder was dissolved in 3 mL of n-trioctylphosphine for one hour at 60° C. Once the selenium precursor was prepared, the cadmium compound was developed in a separate flask by combining 2 mmol of cadmium oxide, 7 mL of 1-octadecene, and 1.5 mL of oleic acid at 100° C. When the cadmium oxide was fully dissolved into the solution, the cadmium precursor was rapidly heated to 270° C and the selenium precursor was injected into the mixture. To grow the nanocrystals, the reaction mixture was heated to 300° C for an hour.

At this point, the nanocrystals from the reaction are surrounded by long, organic ligand chains. These longer ligands impede the electrical conductivity of the CdSe nanocrystals. Therefore, it is preferable to reduce the length of the ligands surrounding the nanocrystals or potentially remove them entirely. For the purposes of this paper, it was elected to reduce the length of the ligands through the process of ligand exchange. Ligand exchange is intuitively a substitution of one ligand chain for another. To achieve the shorter ligand length, excess pyridine was introduced to the nanocrystal solution, and the resulting mixture was agitated with a magnetic stirrer placed in the solution and a stir plate. The solution was vigorously stirred for 10 hours at 70° C in a nitrogen gas atmosphere. The nitrogen gas atmosphere was provided by using a glovebox. To separate the excess solvents from the nanocrystals (with shorter ligands),

the well-stirred solution was dried for several hours – overnight – under vacuum. The dried nanocrystals were then added to chloroform and dispersed in the solution via sonication.

## B. Synthesis of the CuInS<sub>2</sub> Nanocrystals

As is the case with the CdSe nanocrystals, the production of copper indium sulfide nanocrystals is a fairly complicated, multi-step process. In a three neck flask, 292 mg of the indium precursor, indium (III) acetate, is added to 190 mg of the copper precursor, copper (I) iodide, 5 mL of dodecanethiol (DDT) in a three-necked flask. The flask containing the reaction agents is then vacuumed while nitrogen gas (N<sub>2</sub>) was introduced into the flask from a separate tube. The solution is stirred under this nitrogen environment for approximately two hours. At this point, the reaction atmosphere is chemically inert, and the reaction mixture is rapidly heated to 230° C in a 2 minute interval, and the reaction temperature is maintained for 30 minutes. At this point, the contents of the reaction are cooled back to room temperature with a blow-dryer. The experimental set-up is illustrated in Figure 1.

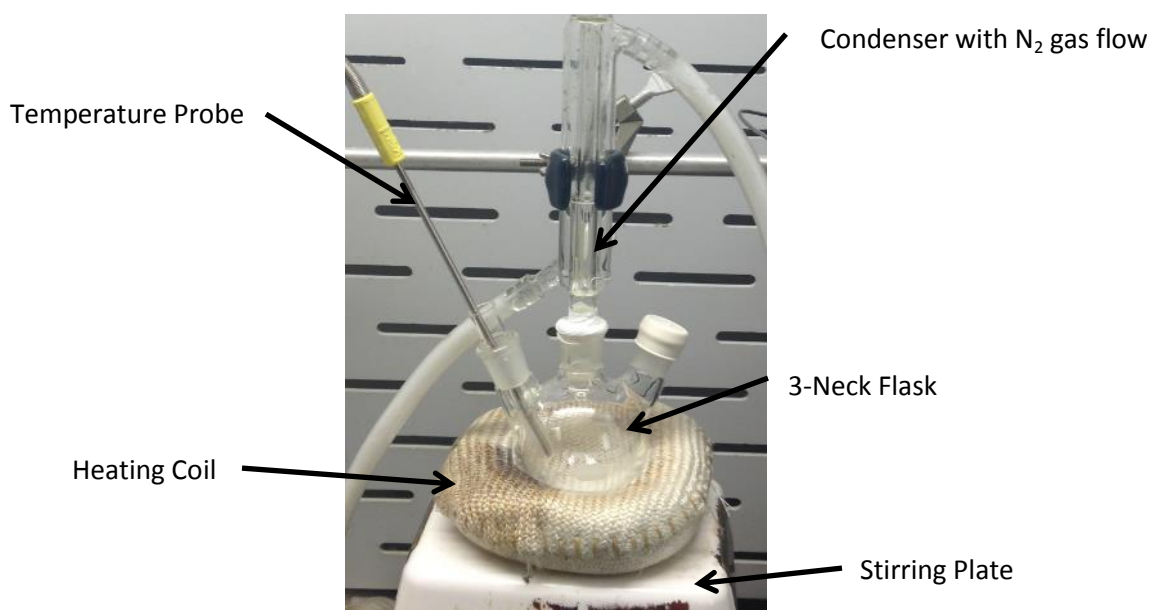


**Figure 1.** Experimental set-up for synthesis

To purify the resulting solution, 2 mL of the solution is added to excess acetone and vigorously agitated. The new solution containing the acetone is then spun in a centrifuge at 6000 rpm for 5 minutes to separate the precipitated nanocrystals from the supernatant. The precipitate is then redispersed in acetone, and centrifuged again for 5 minutes at 6000 rpm. The supernatant is discarded, and the precipitate is dispersed in hexane. The new solution contains the CuInS<sub>2</sub> nanocrystals.

### C. Characterization of the Nanocrystals

The effect of the length of the reaction duration can be seen in Figures 2 and 3 as the samples were extracted from the CuInS<sub>2</sub> reaction mixture at various points throughout the process. The color change is the result of a phenomenon called nucleation, and it matches the results reported in previously literature (Booth, 2012). Figure 3 is perhaps the most obvious way to determine the presence of nanocrystals; as the solution is exposed to ultraviolet light, the solutions containing nanocrystals experience luminescence.

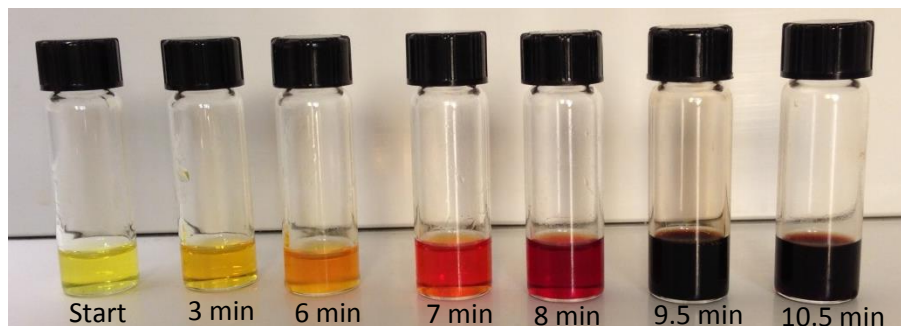


**Figure 2.** Samples extracted from reaction at various times



**Figure 3.** Samples from Figure 1 under Exposure to UV Light

Figure 4 is a graph of the absorbance of the reaction solutions extracted at different points in the reaction process. The graph illustrates that the bandgap is changing with time, decreasing with increased reaction time. Again, this is due to the increasing size of the nanocrystals formed during the reaction.

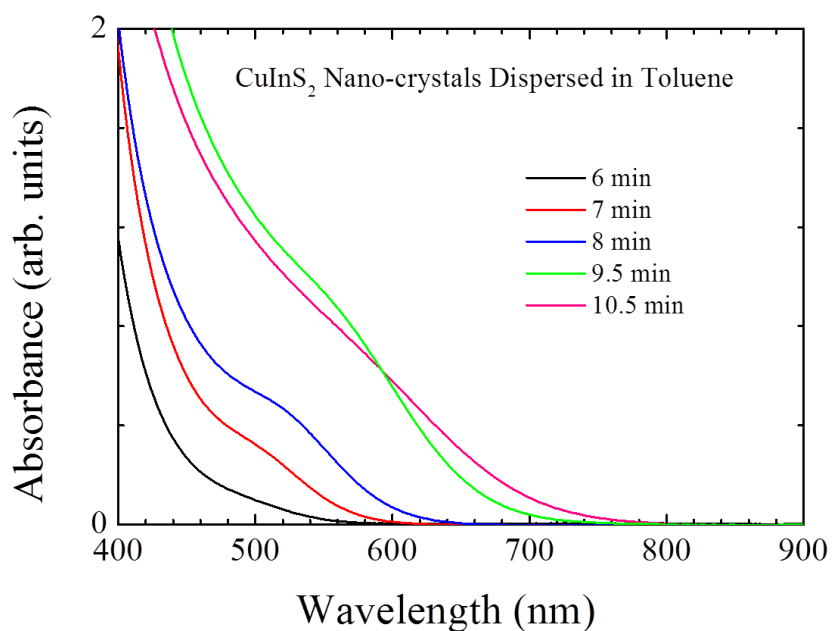


**Figure 4.** Absorbance spectra of samples taken at different reaction times

Figure 5 illustrates the absorbance and the photoluminescence spectra of the CuInS<sub>2</sub> nanocrystals dispersed in toluene. Both the absorbance and the photoluminescence measurements allow one to determine the bandgap of the nanocrystals. The peak of the photoluminescence occurs at 780 nm, and the absorbance spectra threshold is approximately the same. To calculate the bandgap for a given wavelength, one must solve for  $E$  in Equation 1 where  $E$  is in eV, and  $\lambda$  is the wavelength in  $\mu\text{m}$ ; doing so with  $\lambda = .780 \mu\text{m}$  yields approximately  $E = 1.6 \text{ eV}$ .

$$E(\text{eV}) = \frac{1.24}{\lambda(\mu\text{m})} \quad (1)$$

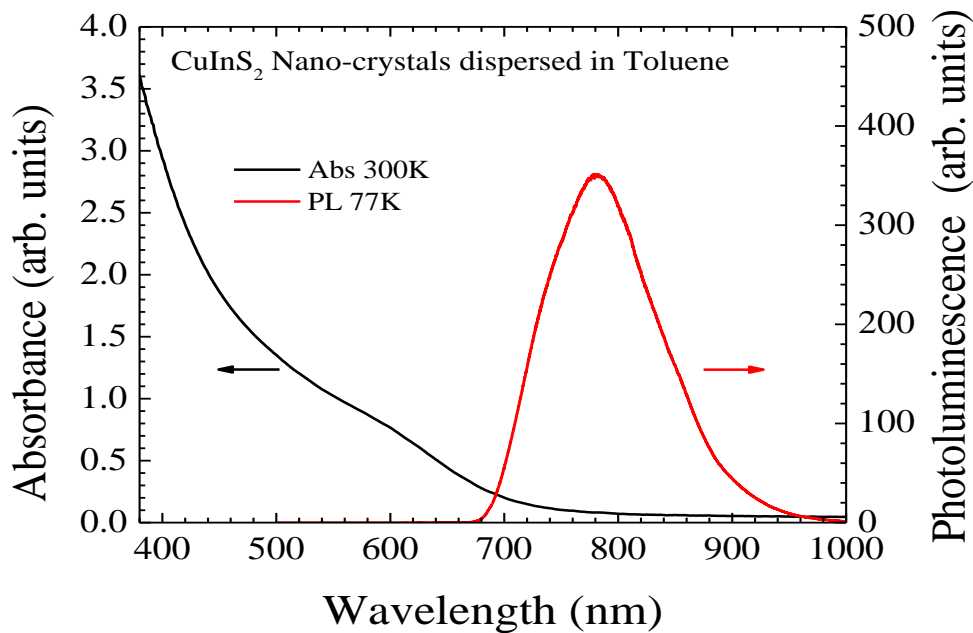


**Figure 5.** Absorbance and photoluminescence spectra

As was the case with the CuInS<sub>2</sub> nanocrystals, varying the reaction time of the CdSe nanocrystals altered their bandgap as the size of the nanocrystals varied. From the graph of the absorbance spectra in Figure 6, it is easy to see that the threshold is shifting to higher

wavelengths corresponding to a decrease in the bandgap as the size of the nanocrystals is increasing throughout the reaction.

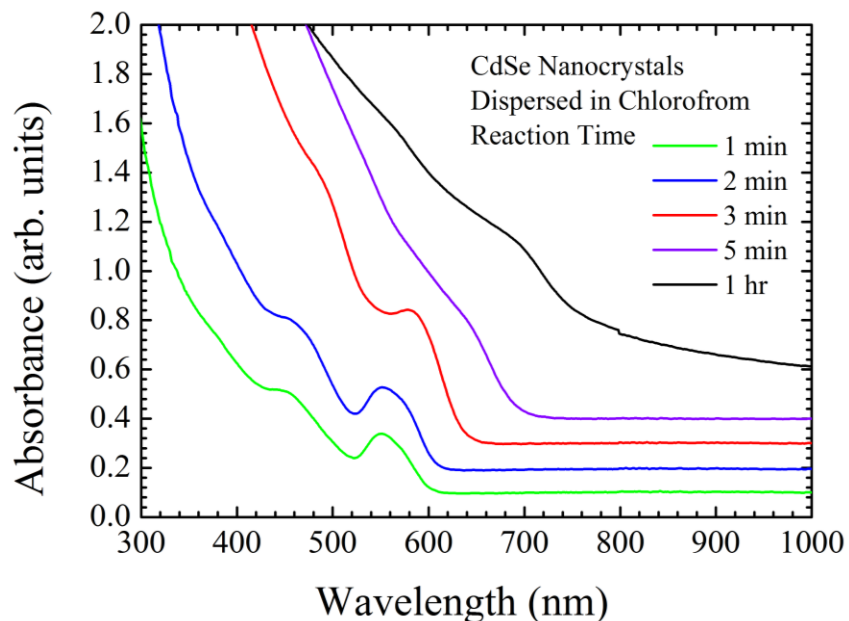


**Figure 6.** Absorbance of CdSe nanocrystals taken at different points in reaction

Figure 7 is the photoluminescence measurements obtained from the CdSe nanocrystals. As with the absorbance spectra, the photoluminescence spectra were taken of samples extracted at different times throughout the reaction. The photoluminescence peaks provide a more definitive approximation of the bandgap of the nanocrystals than absorbance because the bandgap is indicated by the peaks of the graph rather than attempting to estimate where the threshold lies. Upon comparing Figures 6 and 7, it would appear that the graphs are not in agreement as the absorbance spectra indicates a higher bandgap (and lower wavelength) than the photoluminescence does. However, this difference can be attributed to the Stokes Shift phenomenon. The absorbance essentially measures the bandgap as electrons are energized by incident light and jump to the conduction band, while the photoluminescence obtains the

bandgap when the electron falls back to the valence band from the conduction band. The energy required to jump to the conduction band should be the same energy released when an electron falls back to the valence band. However, the energy radiated takes two forms, as light in the form of photons and as lattice vibrations called phonons. The photoluminescence can only capture the energy associated with the photons. As such, if the radiation only took the form of photons, then the absorbance and the photoluminescence would match perfectly. However, since some of the energy instead takes the form of lattice vibrations (phonons), the photoluminescence measures a smaller bandgap (and higher wavelength) than the absorbance measurements.

(Manasreh, 2012)

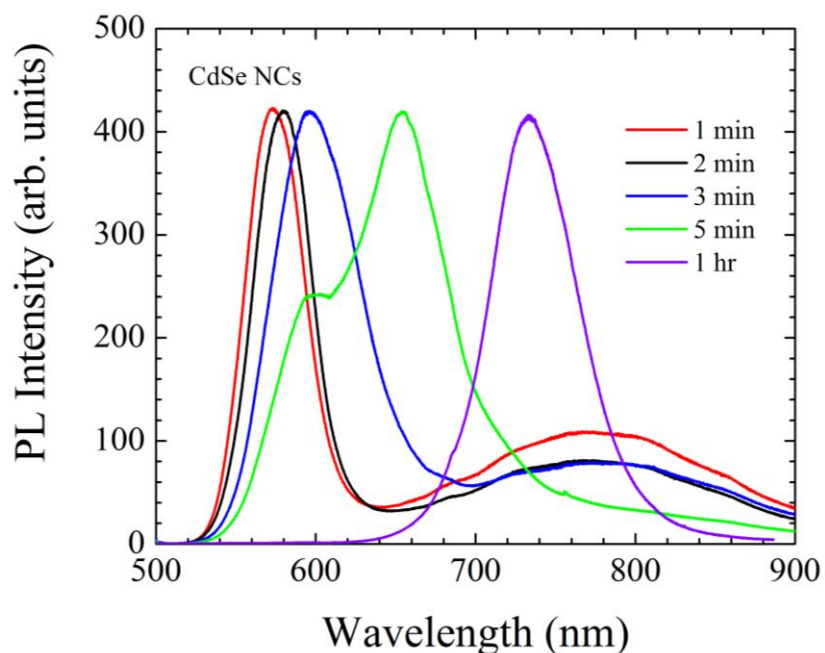


**Figure 7.** Photoluminescence spectra of CdSe nanocrystals



#### **D. Applications: Fabrication of a Nanocrystals-Based Photodetector**

Cadmium selenide nanocrystals are a common choice in the fabrication of nanocrystal-based photodetectors. The field of photodetectors has so far proven an excellent application for cadmium selenide nanocrystals. To this end, after the nanocrystals had been characterized, they were also employed in the production of a photodetector.

The topography of the photodetector is best served as the topic of another paper. However, it is necessary to at least briefly describe the form of the photodetectors. The template was two electrically isolated electrodes separated by a channel. The electrically insulating substrate was glass, and the metal contacts were gold. In an effort to improve device performance, the channel was an interdigital design as illustrated in Figure 8 (Konstantatos, 2006). The nanocrystals were then deposited in the channel by spincoating them at 2000 rpm for 30 seconds. The contacts were then cleaned with acetone.

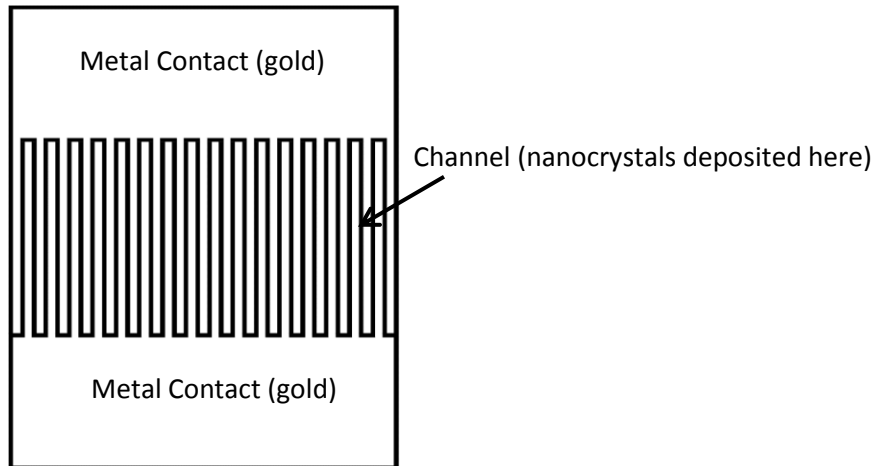


**Figure 8.** Photodetector Design

The channels were made in 2 sizes: 5  $\mu\text{m}$  and 50  $\mu\text{m}$ . The width of the metal contact “fingers” was two times the width of the channels. As the channel width decreased, the detectivity of the device improved as evidenced in the following figures.

Figure 6 is the I-V curve for the CdSe photodetectors. The dark current is simply the current flow between the metal contacts as the device is biased across a range of voltages when the device is shielded from incident light. The photo current is the current flow achieved when the sample is exposed to a light source of a given power. These currents are critically important in determining the efficacy of the photodetector device, as they greatly influence one of the primary figures of merit, the detectivity.

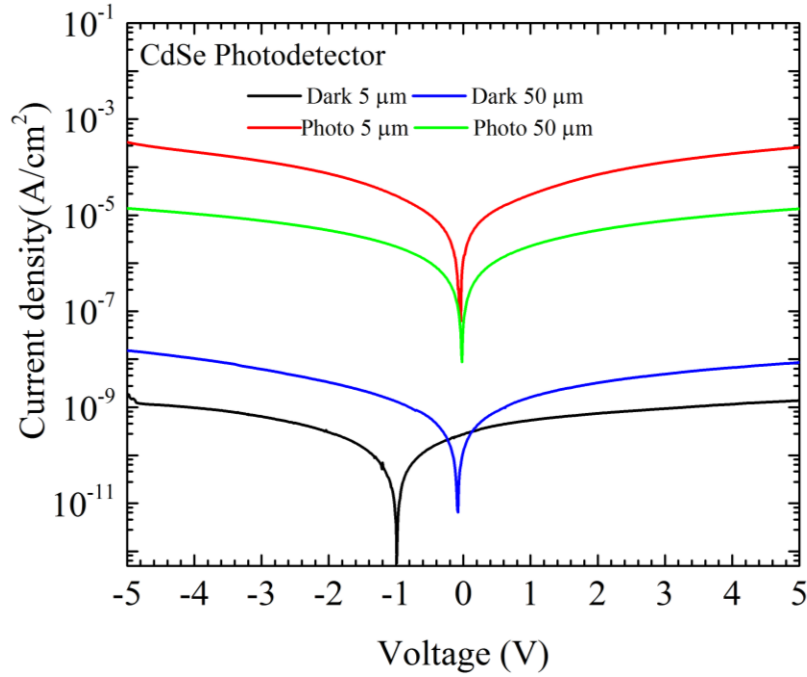


**Figure 9.** I-V curves for 5 and 50 micron channel photodetectors

The equation to calculate the specific detectivity,  $D^*$ , of a photodetector is shown in Equation 2

$$D^* \approx \frac{\sqrt{A}i_{ph}}{\sqrt{2eI_d}P_s} \quad (2)$$

where  $A$  is the active area of the photodetector,  $i_{ph}$  is the photocurrent,  $e$  is the charge of an electron,  $i_d$  is the dark current, and  $P_s$  is the power of the input optical signal (Liu, 2005). The active area for the 5  $\mu\text{m}$  detector was  $0.03 \text{ cm}^2$  and for the 50  $\mu\text{m}$  device, it was  $0.05 \text{ cm}^2$ . The intensity of the light source was  $0.35 \text{ Wcm}^{-2}$ . With this information, it is possible to calculate and plot the detectivity of the devices using the I-V curves from Figure 9.

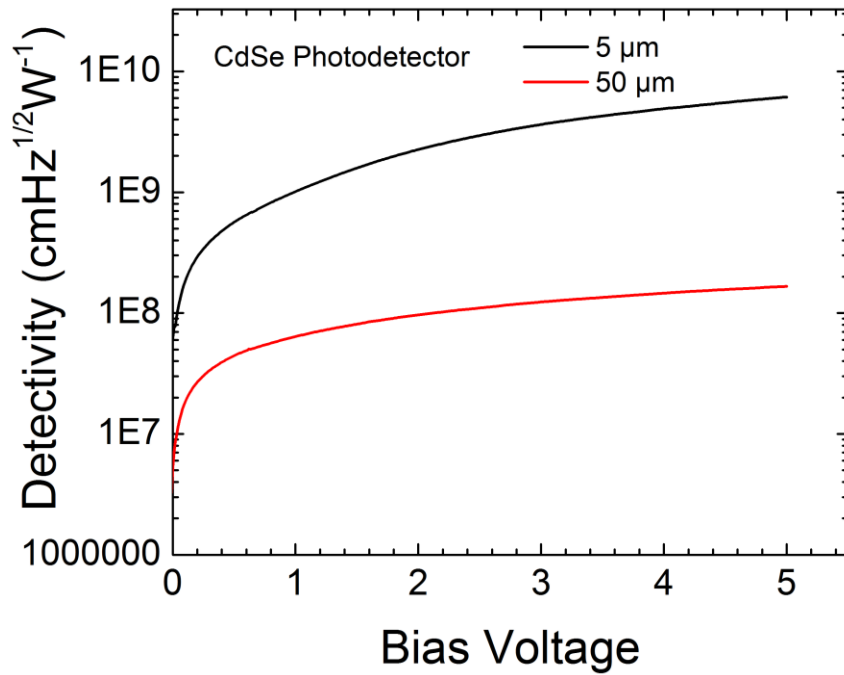


**Figure 10.** Detectivity of 5  $\mu\text{m}$  and 50  $\mu\text{m}$  photodetectors

From Figure 10, it is clear to see that the 5  $\mu\text{m}$  device is better than the 50  $\mu\text{m}$  device. The 5  $\mu\text{m}$  photodetector is anywhere from 1 to 1.5 orders of magnitude better than the larger device. At their highest detectivities (obtained at a bias of 5 V), the smaller device was approximately  $6.12 \times 10^9 \text{ cmHz}^{1/2}\text{W}^{-1}$ , and the larger device was  $1.66 \times 10^8 \text{ cmHz}^{1/2}\text{W}^{-1}$ . The improved detectivity can likely be attributed to the smaller channels as they result in a shorter transit time of the charge carriers which in turn affects the photoconductive gain of the device as illustrated by Equations 3 and 4 where  $t_r$  is the transit time,  $d$  is the electrode spacing,  $\mu$  is the

carrier mobility,  $V$  is the bias voltage,  $G$  is the photoconductive gain, and  $\tau$  is the carrier lifetime (Nusir, 2014).

$$t_r = \frac{d^2}{\mu V} \quad (3)$$

$$G = \frac{\tau}{t_r} = \frac{\tau \mu V}{d^2} \quad (4)$$

### III. Conclusions

This paper presented the production of CuInS<sub>2</sub> and CdSe nanocrystals, their characterization, and the application of such nanocrystals with the fabrication of a CdSe nanocrystals-based photodetector. The nanocrystals were grown via wet chemical method resulting in a colloidal solution. The nanocrystals were characterized for their optical properties by absorbance and photoluminescence spectra and for their semiconductor properties by obtaining their I-V curve under light source and shielded from light. The nanocrystals were then applied in the fabrication of photoconductive photodetectors of two sizes, 5  $\mu\text{m}$  and 50  $\mu\text{m}$ . The 5  $\mu\text{m}$  device provided a much better return than the 50  $\mu\text{m}$  device. This was attributed to a shorter transit time of the charge carriers as reported in the literature.

#### IV. Works Cited

Booth, Matthew, et al. "Determining the Concentration of CuIn<sub>2</sub>S<sub>4</sub> Quantum Dots from the Size-Dependent Molar Extinction Coefficient." *Chemistry of Materials* 24.11 (2012): 7. Print.

"Cadmium Compounds (A)." EPA. Environmental Protection Agency, 1 Jan. 2000. Web. 18 Apr. 2014. <<http://www.epa.gov/ttn/atw/hlthef/cadmium.html>>.

Credi, Alberto. "Electrochemical properties of CdSe and CdTe quantum dots." *Chemical Society reviews* 41 ( ): 5728-5743. Print.

Grindle, Steven, Charles Smith, and Steven Mittleman. "Preparation and Properties of CuIn<sub>2</sub>S<sub>4</sub> Thin Films Produced by Exposing Sputtered CuIn Films to an H<sub>2</sub>S Atmosphere." *Applied Physics Letters* 35.1 (1979): 3. Print.

Konstantatos, Gerasimos, et al. "Ultrasensitive Solution-Cast Quantum Dot Photodetectors." *Nature* 442 (2006): 180-83. Print.

Li, Liang, Nelson Coates, and Daniel Moses. "Solution-Processed Inorganic Solar Cell Based on in Situ Synthesis and Film Deposition of CuIn<sub>2</sub>S<sub>4</sub> Nanocrystals." *Journal of the American Chemical Society* 132.1 (2009): 2. Print.

Liu, Jia-Ming. "Photodetectors." *Photonic Devices*. Vol. 1. Cambridge, United Kingdom: Cambridge University Press, 2005. 926-1008. Print.

Manasreh, Omar. "Optical Properties." *Introduction to Nanomaterials and Devices*. Chichester: John Wiley & Sons, Inc., 2012. . Print.

Nusir, Ahmad, Juan Aguilar, Zach Bever, and Omar Manasreh. "Uncooled photodetectors based on CdSe nanocrystals with an interdigital metallization." *Applied Physics Letters* 104 ( ): 1-4. Print.

Searson, Peter C.. "Synthesis of Cadmium Selenide Quantum Dots from a Non-Coordinating Solvent: Growth Kinetics and Particle Size Distribution." *Journal of Physical Chemistry C* 112 ( ): 17849-17854. Print.

"Selenium Compounds." EPA. Environmental Protection Agency, 1 Jan. 2000. Web. 18 Apr. 2014. <<http://www.epa.gov/ttn/atw/hlthef/selenium.html>>.

Web. <<http://www.epa.gov/osw/hazard/wastemin/minimize/factshts/cadmium.pdf>>.

Yang, P., C. Li, and N. Murase. "Highly Photoluminescent Multilayer Qd-Glass Films Prepared by Lbl Self-Assembly " *Langmuir* 21.19 (2005): 5. Print.